Available online at www.sciencedirect.com
ScienceDirect
Journal of Power Sources 173 (2007) 36–44
JOURNAL OF POWER SOURCES
www.elsevier.com/locate/jpowsour

# Sol–gel derived sulfonated-silica/Nafion® composite membrane for direct methanol fuel cell

Chuan-Yu Yen [a], Chia-Hsun Lee [a], Yu-Feng Lin [a], Hsiu-Li Lin [b], Yi-Hsiu Hsiao [a], Shu-Hang Liao [a], Chia-Yi Chuang [a], Chen-Chi M. Ma [a,*]

[a] *Department of Chemical Engineering, National Tsing-Hua University, Hsin-Chu 30043, Taiwan, ROC*
[b] *Department of Chemical Engineering & Materials Science, Yuan-Ze University, Chung-Li, Taoyuan 32003, Taiwan, ROC*

Received 6 July 2007; received in revised form 6 August 2007; accepted 7 August 2007
Available online 14 August 2007

**Abstract**

Sulfonated-silica/Nafion® composite membranes were prepared in a sol–gel reaction of (3-Mercaptopropyl)trimethoxysilane (SH-silane) followed by solution casting, and then oxidated using 10 wt% $H_2O_2$ solution. The chemical and physical properties of the composite membranes were characterized by using FT-IR, XPS, $^{29}$Si NMR and SEM analyses. Experimental results indicated that the optimum oxidation condition was 60 °C for 1 h. The performance of the silica–$SO_3H$/Nafion® composite membranes was evaluated in terms of methanol permeability, proton conductivity and cell performance. The silica–$SO_3H$/Nafion® composite membranes have a higher selectivity (C/P ratio = 26,653) than that of pristine Nafion® (22,795), perhaps because of their higher proton conductivity and lower methanol permeability. The composite membrane with 0.6 wt% silica–$SO_3H$/Nafion® performed better than pristine Nafion®. The current densities were measured as 62.5 and 70 mA cm$^{-2}$ at a potential of 0.2 V with a composite membrane that contained 0 and 0.6 wt% silica–$SO_3H$, respectively. The cell performance of the DMFC was improved by introducing silica–$SO_3H$. The composite membrane with 0.6 wt% of silica–$SO_3H$ yielded the maximum power density of 15.18 mW cm$^{-2}$. The composite membranes are suitable for DMFC applications with high selectivity.


*Keywords:* Sol–gel; (3-Mercaptopropyl)trimethoxysilane; Nafion®; DMFC; X-ray; $SiO_2$–$SO_3H$

## 1. Introduction

Fuel cells are promising power sources because of their high energy density and environmental protection. Among the numerous fuel cells, direct methanol fuel cells (DMFCs) are especially attractive as portable power sources. However, methanol crossover is a major problem that limits its range of practical applications [1]. The fluorinated membrane Nafion® from DuPont Co. has been widely used as a proton-conducting electrolyte membrane because of its excellent chemical, mechanical, thermal stability and high proton conductivity (∼0.1 S cm$^{-1}$). However, Nafion® shows high methanol permeability (∼$10^{-6}$ cm$^2$ s$^{-1}$), which reduces the performance of DMFCs [2]. The challenge is to reduce the methanol crossover and to improve the proton conductivity of the membrane.

Numerous attempts have been made to reduce the methanol permeability through polymer electrolyte membranes. They include (i) modifying the surface of the Nafion® membranes to block the methanol transport [3–8]; (ii) developing new electrolyte polymers [9]; and (iii) introducing a winding pathway for a methanol molecule by preparing a composite with inorganic materials [10–18]. Most composite membranes have been prepared by adding a nonconductive ceramic oxide, such as silica [10,11], zirconia [12], titania [13], organo-montmorillonite [14] and such proton-conductive materials as sulfonated montmorillonite [15–17] and sulfonated phenethyl-silica [18] into the Nafion® membrane. When applied to DMFCs, these composite membranes reduce methanol crossover. However, this effect

* Corresponding author. Tel.: +886 3571 3058; fax: +886 3571 5408.
*E-mail address:* ccma@che.nthu.edu.tw (C.-C.M. Ma).

0378-7753/$ – see front matter © 2007 Published by Elsevier B.V.
doi:10.1016/j.jpowsour.2007.08.017

does not always provide the desired improvement in the performance of the membrane-electrode assembly (MEA), mainly because the proton conductivity of the composite membranes that are fabricated with these less proton-conductive oxides was much lower than that of the pristine Nafion® membrane.

Several Nafion®/silica hybrid composite membranes have been recently prepared by the sol–gel reaction of tetraethoxysilane (TEOS) to form silica in the membrane [19–21]. Deng et al. [22] described the possibility of using Nafion®/silica hybrid membrane in a PEM fuel cell with a higher water uptake but lower methanol uptake, and greater mechanical strength than the unmodified Nafion® membrane. Using the same method, Jalani et al. [23] synthesized Nafion®-$MO_2$ (M = Zr, Si, Ti) nanocomposite membranes via the *in situ* sol–gel technique and compared them with the unmodified Nafion®. Nafion®-$MO_2$ (M = Zr, Si, Ti) exhibited good water uptake properties. Furthermore, chemical, physical and thermal properties were improved by incorporating nanosized inorganic additives which have higher acidity and more favorable water uptake properties.

Ren et al. [24] reported the incorporation into Nafion® by various additives that have been grafted with organic functional groups, including 5 wt% of mercaptopropylmethyldimethoxysilane $HS(CH_2)_3CH_3Si(OCH_3)_2$ (–SH), TEOS and $HS(CH_2)_3CH_3Si(OCH_3)_2$-TEOS (TEOS–SH). After oxidation, the composite membranes were oxidized with $H_2O_2$ solution and, then, the thiol (–SH) group was converted to a sulfonic group (–$SO_3H$). The proton conductivity of the composite membranes decreased slightly and the methanol permeability was reduced. Rhee et al. [25] oxidized the thiol functional group to sulfonic groups by 10 wt% $H_2O_2$ at different temperatures and the membrane was characterized by X-ray photoelectron spectra (XPS). However, the DMFC test using these composite membranes underperforms pure Nafion® because of its inadequate. Hence, the purpose of this study is to find out the optimized oxidized conditions under which silica–SH/Nafion® composite membrane is suitable for DMFC.

In this investigation, the silica–SH/Nafion® composite membranes were prepared by *in situ* sol–gel reaction. The properties of the oxidized membranes with different quantities of additives were compared. The silica network in the silica–SH/Nafion® composite membrane was analyzed by $^{29}$Si NMR and FT-IR. The oxidation contribution was characterized by XPS. The composite membranes derived from Nafion®/silica–$SO_3H$ exhibit improved performance. In this work, the proton conductivity, the methanol permeability and the single cell performance were studied and compared with those of pristine Nafion®.

## 2. Experimental section

### 2.1. Membrane preparation

(3-Mercaptopropyl)trimethoxysilane (SH-silane) was introduced into a beaker with methanol (99.9%, Aldrich Co. Fairfield, OH, USA) to prepare SH-silane/methanol diluted solutions. The quantity of SH-silane and Nafion® solution was varied to obtain different $SiO_2$ contents (0.3–1.2 wt% based on Nafion®) in the membrane. The solutions were further stirred for 1 h at room temperature for sol–gel reaction. The mixture prepared was slowly poured in a glass dish in the quantity that would provide a thickness of ca. 120 μm of the formed composite membrane. The filled glass dish was placed on the leveled plate of a vacuum-dry oven, and then was dried by increasing the temperature slowly from 300 to 323 K to prevent crevice of composite membrane. Finally, the residual solvent in the composite membrane was removed completely by evacuation at 373 K for 12 h. Fig. 1 describes the procedure for preparing the composite membrane. The membranes were oxidized by immersing in 10 wt% $H_2O_2$ solution for 1 h at 337 K and then dried in an oven. The silica–$SO_3H$/Nafion® composite membranes was prepared.

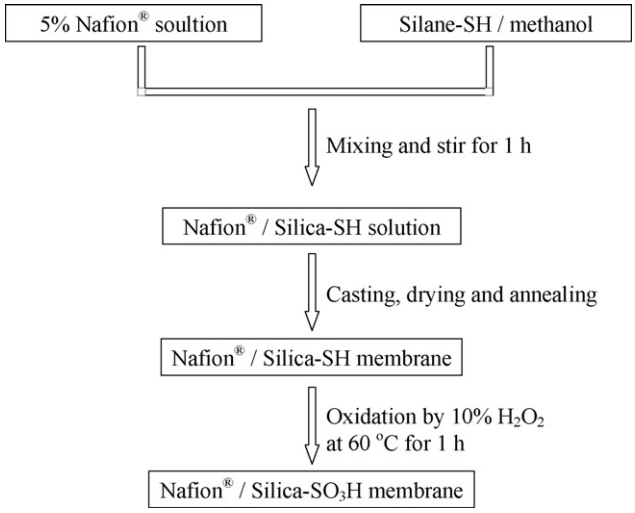


Fig. 1. The process for preparing the silica–$SO_3H$/Nafion® composite membranes.

### 2.2. Characterization

FTIR spectra of the silica–SH/Nafion® composite membranes, were recorded between 1400 and 500 $cm^{-1}$, on a Nicolet Avatar 320 FT-IR spectrometer (USA). The polymer solutions were casted onto the KBr pellet, and then dried 5 min to evaporate the solvent. A minimum of 32 scans was signal-averaged with a resolution of 1 $cm^{-1}$ in the 1400–500 $cm^{-1}$ range.

The thiol (–SH) transformed to sulfonic (–$SO_3H$) groups was analyzed by X-ray photoelectron spectra (XPS) acquired with a VG-Scientific ESCALAB 220 iXL spectrometer and equipped with a hemispherical electron analyzer and an Mg Kα ($h\nu$ = 1253.6 eV) X-ray source. Solid state $^{29}$Si NMR experiments were performed on a Brüker DSX-400 Spectrometer. The $^{29}$Si NMR was used to characterize the structure of silica. The morphology of the composite polymer membranes was investigated using a scanning electron microscope (JEOL-6300F).

### 2.3. Ionic exchange capacity measurement

The quantity of acid equivalents per gram of polymer can be obtained by the following steps. First, the membrane in the acid form was immersed in 2 M NaCl solution to convert sulfonic acid to sodium form. Next, the released $H^+$ was back titrated

with a 0.01N NaOH solution using phenolphthalein as indicator, meanwhile, the volume of NaOH and pH was recorded to determine the equivalence point. The IEC is the equivalents per gram of dry polymer.

### 2.4. Water uptake and swelling

Polymer membranes were dried in a vacuum oven at 80 °C for 2 h and weighted. Then the sample was immersed in distilled water and isothermal oscillating at 60 °C for 2 h. The water uptake was calculated using the following equation:

$$\text{Water uptake } (\%) = \frac{W_{\text{wet}} - W_{\text{dry}}}{W_{\text{dry}}} \times 100 \quad (1)$$

where $W_{\text{wet}}$ is the weight of wet membranes and $W_{\text{dry}}$ is the weight of dry membranes.

### 2.5. Proton conductivity and methanol permeability measurement

Proton conductivities of membranes were measured at room temperature by AC impedance method, a Solartron Interface 1260 gain phase analyzer Hampshire, U.K. was used, over the frequency range of 10 kHz–1 Hz. The sample was sandwiched between two circular platinum electrodes of 1.0 mm diameter in an open cell. The conductivity was calculated from the following equation: $\sigma = L/RA$, where $L$ is the membrane thickness, $A$ the surface area of the electrodes and $R$ is the membrane resistance. Methanol permeability was determined and calculated by using two connected compartment cells as described in our previous paper [14]. In the beginning, one compartment was filled with 10 M methanol solution, and the other compartment was filled with deionized water. Each compartment was kept stirring during experiment to ensure the uniformity of the cell concentration. The refractive index of methanol solution was recorded with time and was converted to the methanol concentration. Methanol permeability was obtained by analyzing the methanol concentration with time.

### 2.6. Membrane-electrode assembly (MEA) fabrication and fuel cell evaluation

The membranes were immersed in 1 M sulfuric acid for 1 day and then washed with distilled water to remove the remaining sulfuric acid in order to assure of the hydrogen form of the composite membranes. Fuel cell experiments were carried out in a 2 cm × 2 cm self-designed single cell as described in our previous paper [26]. The single-cell was tested with 5 M methanol solution and air breathing after equilibrium at 40 °C for 4 h. A layer of 20 wt% of PtRu (1:1 a/o) on carbon black (anode) and 20 wt% of Pt on carbon black (cathode) were applied on two gas diffusion layers. The content of catalyst loading was approximately 0.2 and 0.5 mg cm$^{-2}$ for anode and cathode, respectively.

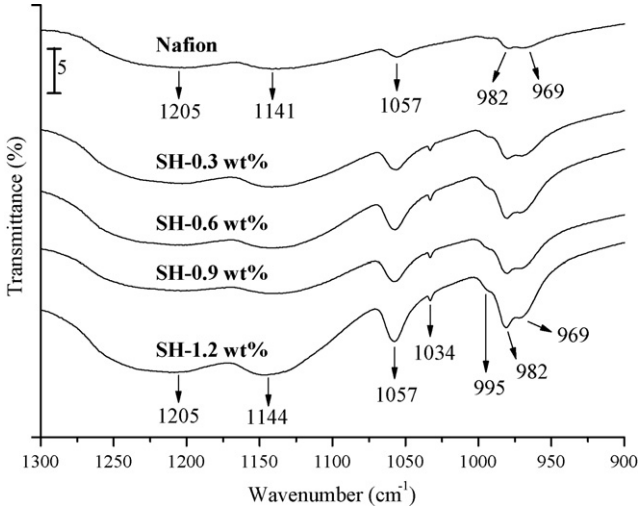


Fig. 2. FT-IR spectra of pristine Nafion® and composite silica–SH/Nafion® membranes.

## 3. Results and discussion

### 3.1. FT-IR analysis of the microstructure of composite membrane

Fig. 2 illustrates the FT-IR spectra, which include the IR absorbance features that are related to the molecular structure of silica–SH/Nafion® composite membranes. The signature peaks are characteristic of silicate structures. Mauritz [27] assigned these peaks for silicate nanostructures that are generated by an *in situ* sol–gel process in Nafion® membranes. In these spectra, the peaks of the pristine Nafion® bands appeared at 969, 982, 1057 cm$^{-1}$ and a broad band existed from 1100 to 1300 cm$^{-1}$. After the silica–SH was added, new absorption wavenumbers of the silica–SH, 995 and 1034 cm$^{-1}$, appeared, as shown in Table 1. The absorption peak at 995 cm$^{-1}$ was due to the symmetric stretching vibration of the Si–O–Si groups, providing evidence of a successful condensation reaction between Si–OR groups. This absorbance peak increased with the silica loading from 0.3 to 1.2 wt%. The peak at 1034 cm$^{-1}$ increased slightly with the silica content in the composite membrane, which trend was attributed to the Si–OH stretching vibration. The Si–OH band represents the incomplete condensation of Si–OH groups and is sometimes referred to as a "defect band" within the silica network structure [28]. The silica–SH clearly was successfully introduced into the Nafion® membrane.

Table 1
Comparison of IR frequencies (cm$^{-1}$) of Nafion® and silica–SH/Nafion® membranes[a]

| Pristine Nafion® (this work) | Silica–SH/Nafion® (this work) | Assignment (Refs. [4,31,32]) |
|---|---|---|
| 969,982 | 969,982 | υ (C–O–C) |
| | 994 | υ (Si–O–Si) |
| | 1034 | ρ (Si–OH) |
| 1057 | 1057 | υ (–$SO_3$H) |
| 1100–1300 | 1100–1300 | υ (C–F) |

[a] υ: stretching; ρ: deformation.

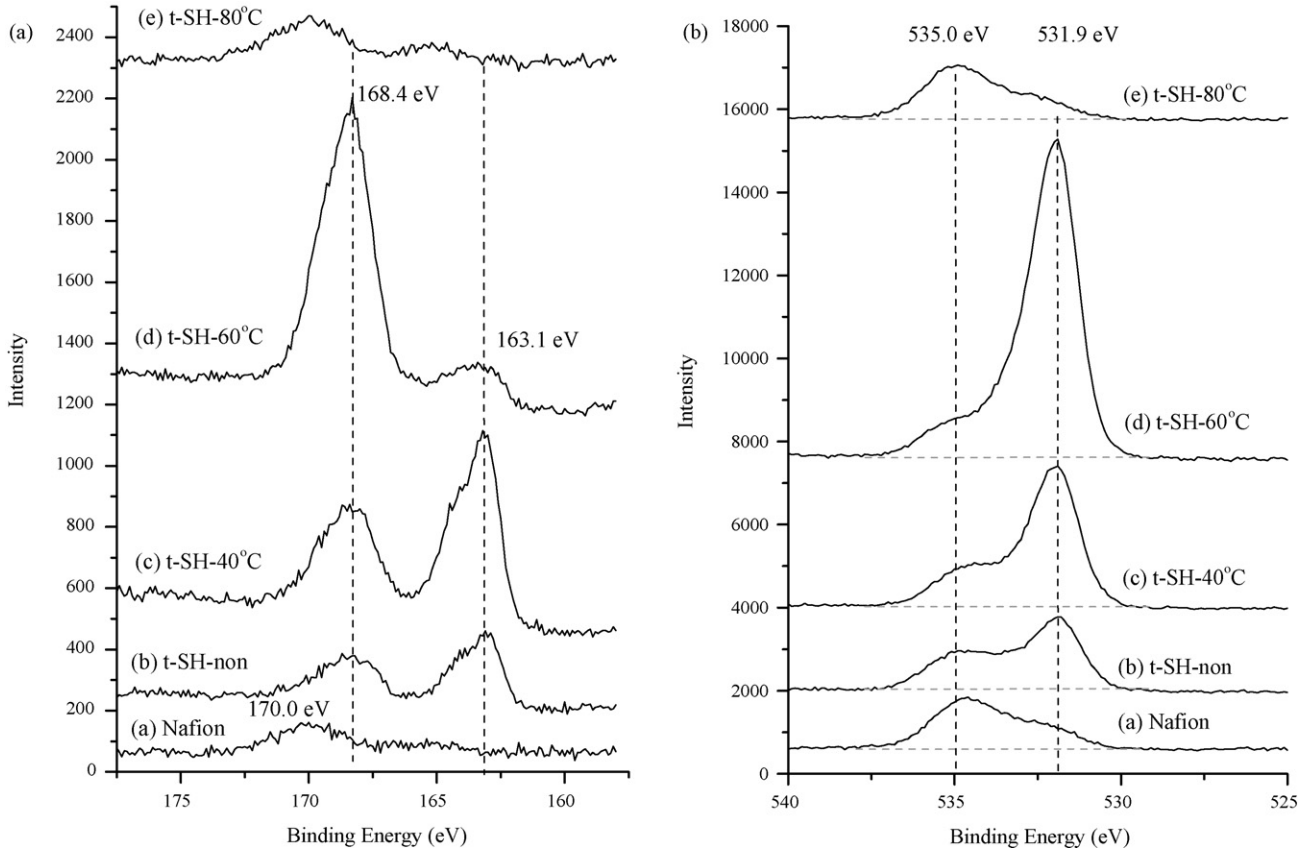


Fig. 3. High-resolution XPS spectra of the surface of Nafion® and Nafion® composite membranes: (a) S2p; (b) O1s oxidation for 1 h at various temperatures.

### 3.2. X-ray photoelectron spectra

The optimum oxidative conditions were examined using X-ray photoelectron spectra (XPS), which revealed the degree of oxidation of thiol (–SH) to sulfonic acid (–$SO_3H$) groups at different temperatures (40, 60, 80 °C) at the same time (1 h), as shown in Figs. 3 and 4. In Fig. 3(a), the XPS of the S2p core level for the *in situ* outgassed samples revealed characteristic $S2p_{3/2}$–$S2p_{1/2}$ spin-orbit splitting. The chemical characteristics of the samples should be taken into account from the more intense component of $S2p_{3/2}$. The 1.2 wt% silica–SH/Nafion® composite membrane consists of two sulfur species: one has a low binding energy (BE) (162.0–163.3 eV), which corresponds to a thiol (–SH) group, and the other has a higher BE (168.3–171.0 eV), which is associated with the sulfonic acid (–$SO_3H$) group [29]. This energy difference in the XPS analysis is useful in evaluating the degree of oxidation of thiol to sulfonic groups near the surface region. As plotted in curve (d) in Fig. 3(a), ca. 90% of thiol groups were converted to sulfonic groups at an oxidation temperature of 60 °C, based on curve fitting. Only 8–10% of the thiol groups remained unoxidized. However, all functionalized sulfur groups were detached from the surface when the reaction was preformed at an uncontrolled reaction temperature (80 °C), as revealed by curve (e) in Fig. 3(a). Additionally, curve (c) in Fig. 3(a) reveals only 40% –SH conversion to –$SO_3H$ groups in the membrane. This result indicates that controlling the oxidation conditions (time, temperature) is very important in minimizing the detachment of the functionalized thiol groups on the surface of silica and in completing the conversion of –SH to sulfonic acid groups. However, the total amount of sulfur remained only ca. 90% of the initial sulfur content of the sample after oxidation. This result can be compared with that for the non-treated membrane (t-SH-non), obtained from curve (b) in Fig. 3(a).

The O1s high-resolution spectrum of the unmodified Nafion® exhibits two peaks centered at 535.0 and 532.5 eV, which may be attributed to the oxygen atom on the ether linkage and the oxygen atom on the sulfonic acid group, respectively, as shown in curve (a) of Fig. 3(b) [29]. In the presence of silica–SH, the shape of the O1s peak changes and the overall atomic percentage increases. These results were reasonable since the O1s peak reveals the appearance of a new component in the presence of silica–SH/Nafion® composite membrane, as shown in curve (b) of Fig. 3(b). A peak that appears at 531.9 eV is attributable to the oxygen atom on the silica network, synthesized in a sol–gel reaction. This peak overlaps the position of the sulfonic acid oxygen of Nafion®. The experimental conditions of curves (c)–(e) of Fig. 3(b) are the same as those in Fig. 3(a). Curve (d) of Fig. 3(b) is associated with the optimum oxidized conditions. In Fig. 4(a) and (b), the samples with different oxidation times at the same temperature (60 °C) are compared. The figures suggest that the optimum oxidation conditions were 60 °C for 1 h.

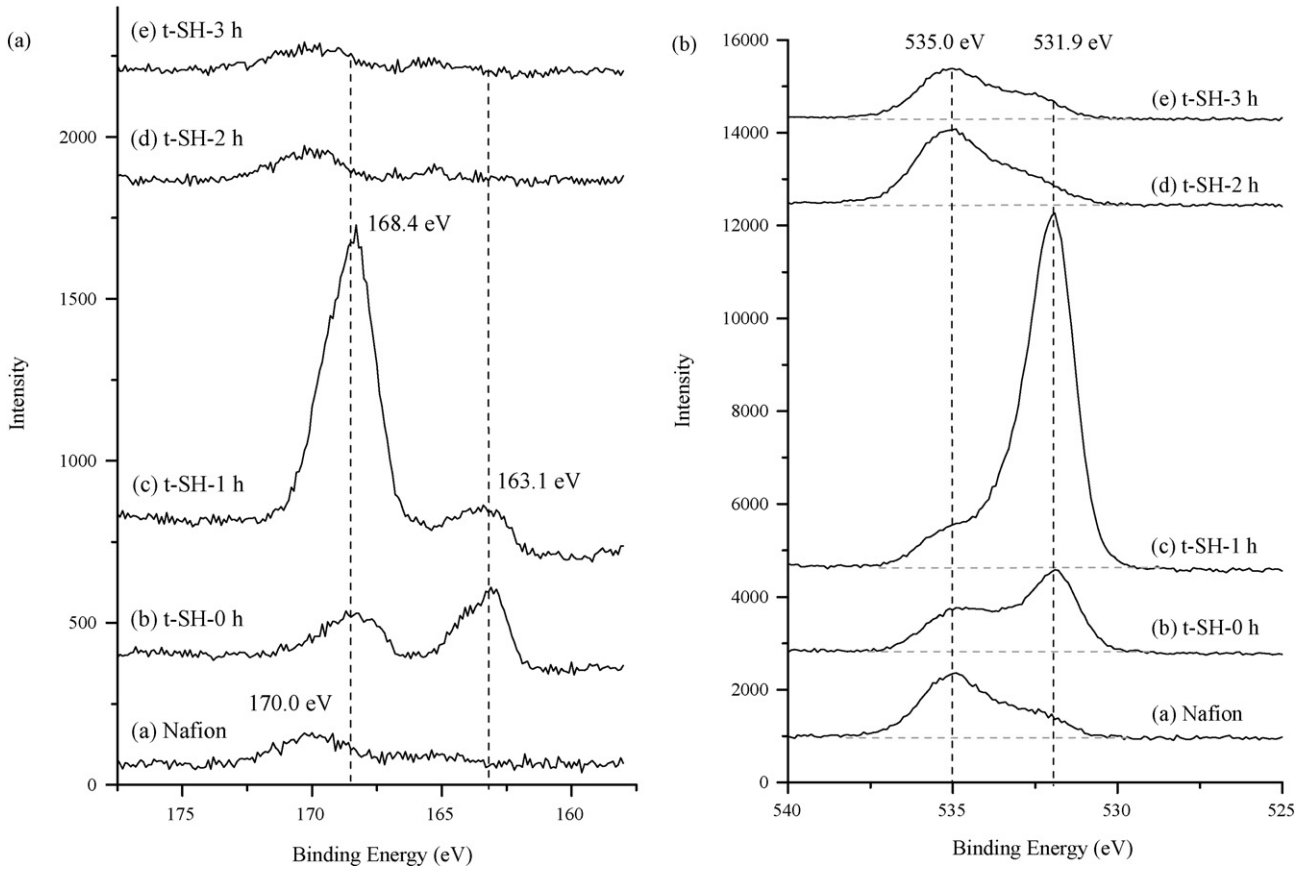


Fig. 4. High-resolution XPS spectra of the surface of Nafion® and Nafion® composite membranes: (a) S2p; (b) O1s oxidation at 60 °C for various times.

### 3.3. $^{29}$Si nuclear magnetic resonance

$^{29}$Si NMR spectroscopy is an excellent tool for studying the structure of silicates, silica gel and silylated silica gel [28]. Silica gel exhibits $^{29}$Si resonances generally in the range −50 to −70 ppm, as shown in Fig. 5. The resonance $T^3$ is attributed to the central Si atom in the (–$CH_2$–) Si (–OSi–)$_3$ species and the $T^2$ resonance represents the central Si in (–$CH_2$–) Si (–OSi–)$_2$(–$OCH_3$).

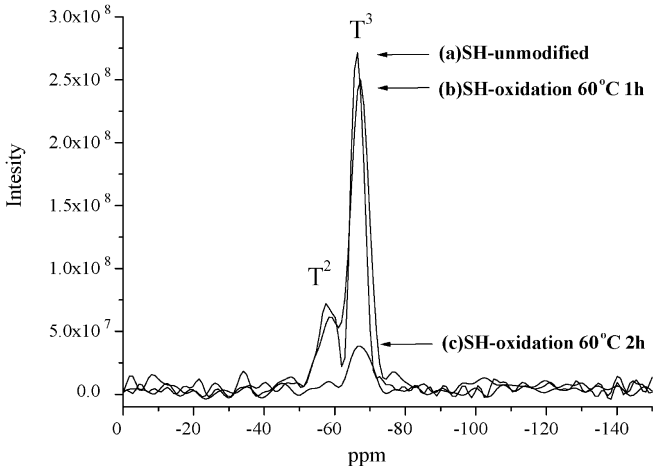


Fig. 5. $^{29}$Si NMR spectra of silica–SH/Nafion® oxidized at 60 °C at various time.

Table 2 summarizes the $^{29}$Si composition of a sol–gel derived silica–SH/Nafion® composite membrane. The results indicate that the silica nanostructures were generated by an *in situ* sol–gel process, as shown in curve (a) of Fig. 5. They are consistent with results of FT-IR described above. When silica–SH was treated with 10 wt% $H_2O_2$ solution to oxidize the thiol group, the intensity of the original peak (*T*) declined slightly, indicating that a few grafted molecules were detached from the silica surface. Furthermore, the surfaces of functionalized groups remained, as shown in curve (b) of Fig. 5. However, all functionalized sulfur groups and silica were detached from the surfaces when the oxidation was preformed for an uncontrolled reaction time, as revealed by curve (c) of Fig. 5.

### 3.4. Morphology of composite membranes

The microstructures of pristine Nafion®, silica–SH/Nafion® and silica–$SO_3$H /Nafion® composite membranes were studied using a scanning electron microscope (SEM). Fig. 6 depicts the representative surface images of the samples. The SEM microphotograph (a) of Fig. 6 demonstrates that the neat Nafion® membrane has a homogenous structure. Fig. 6(b) and (c) show membranes with 0.9 wt% silica–SH and 0.9 wt% silica–$SO_3$H particles in the ionomer matrix, respectively. As can be seen clearly from these images, the particulates sizes are 2–3 μm or less. The distribution of the silica particles is relatively homogenous, with differences in the sizes of the additive particles.

Table 2
*T* distribution of silica–$SO_3H$/Nafion® composite membranes

| Sample | $T^2$ (%)[a] | $T^3$ (%)[b] |
|---|---|---|
| (a) SH-unmodified | 24 | 80 |
| (b) SH-oxidation 60 °C, 1 h | 20 | 76 |
| (c) SH-oxidation 60 °C, 2 h | 5 | 95 |

[a] $T^2$:

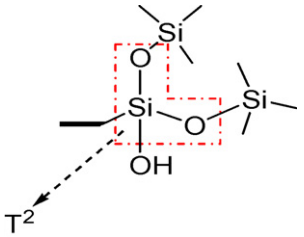


[b] $T^3$:

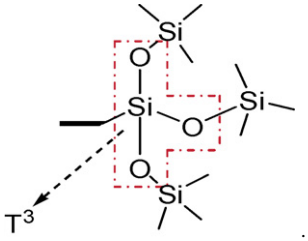


### 3.5. Proton conductivity, water uptake and swelling

The water uptake and swelling are very crucial in DMFC because they are closely related to the proton conductivity and the mechanical strength of the proton-conducting membrane. Hybridizing Nafion® with various amounts of silica–SH reduces the water uptake and the swelling of the membranes, as shown in Table 3. The slight decrease in the water uptake and swelling may be associated with the introduction of the hydrophobic materials (such as silica–SH). After oxidizing by 10 vol.% $H_2O_2$, the water uptake and swelling of silica–$SO_3H$/Nafion® composite membrane were slightly higher than that of silica–SH/Nafion®. The terminal functional group (–$SO_3H$) of silica–$SO_3H$ was hydrophilic, and will associated with the hydrated species. Fig. 7 presents the effect of silica–SH and silica–$SO_3H$ content on the proton conductivity of Nafion® composite membranes. In the proton conductivity experiment, each sample was measured more than five times. Every result was averaged in the error range ±5%. The proton conductivity of silica–SH/Nafion® composite membranes declined as the silica–SH content increased, perhaps because the silica particles were embedded in the cluster of the membrane and block the transfer of protons. Additionally, the proton conductivity of silica–$SO_3H$/Nafion® exceeded that of the silica–SH/Nafion® composite membrane. The silica–$SO_3H$/Nafion® composite membrane is proposed to have a more hydrophilic sulfonic group than that of silica–SH/Nafion® because of the generation of the –$SO_3H$ group following the oxidation of the –SH group. However, introducing silica–SH into Nafion® would reduce the IEC value and the water uptake of the silica–SH/Nafion® membrane. Moreover, the IEC value of silica–$SO_3H$/Nafion® would increase as the silica–SH/Nafion® membrane was oxidized, as shown in Table 3. However, the proton conductivity of the silica–$SO_3H$/Nafion® membrane does not increase linearly with the silica content over 0.6 wt%, perhaps because of slight phase separation.

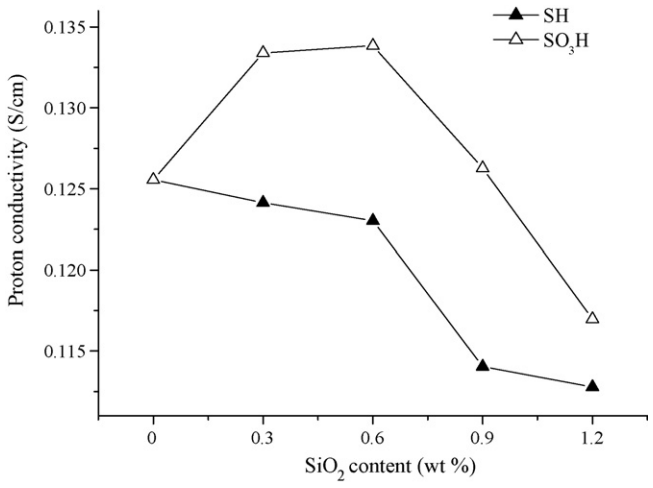


Fig. 7. Proton conductivities of silica–$SO_3H$/Nafion® and silica–SH/Nafion® on the various contents.

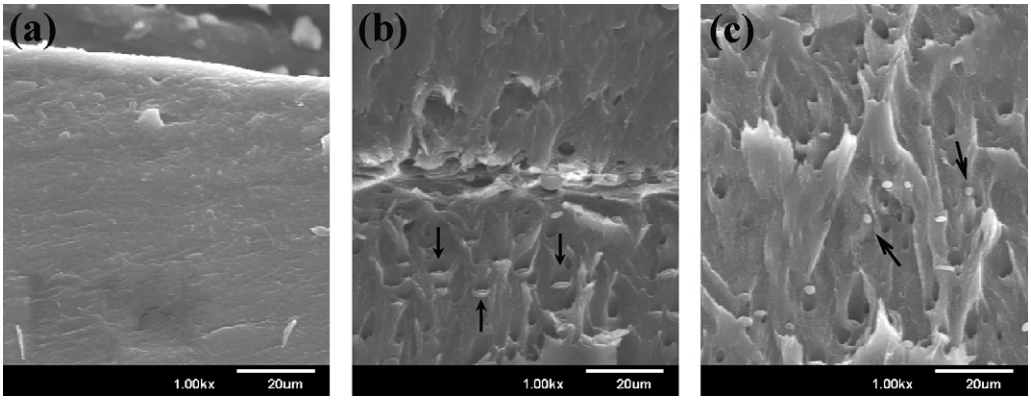


Fig. 6. Microphotographs of (a) pristine Nafion® (b) 0.9 wt% silica–SH/Nafion® (c) 0.9 wt% silica–$SO_3H$/Nafion®.

Table 3
Physical properties of silica–$SO_3H$/Nafion® composite membranes

| Sample | IEC (mmol/g)[a] | $\sigma$ (mS cm$^{-1}$) | $P$[b] ($\times10^{-6}$ cm$^2$ s$^{-1}$) | C/P ratio ($\times10^4$) | Water uptake[c] (%) | Swelling[c] (%) |
|---|---|---|---|---|---|---|
| Pristine Nafion® | 0.949 | 125.6 | 5.51 | 2.28 | 80.45 | 19.73 |
| 0.3 wt% silica–$SO_3H$/Nafion® | 0.976 | 133.4 | 5.23 | 2.55 | 76.11 | 19.05 |
| 0.6 wt% silica–$SO_3H$/Nafion® | 0.980 | 133.8 | 5.02 | 2.67 | 71.46 | 18.71 |
| 0.9 wt% silica–$SO_3H$/Nafion® | 0.987 | 126.3 | 4.86 | 2.60 | 69.16 | 17.87 |
| 1.2 wt% silica–$SO_3H$/Nafion® | 1.011 | 117.0 | 4.71 | 2.48 | 62.22 | 17.34 |

[a] A base-titration procedure measures the equivalents of sulfonic acid in the polymer, and the method was used to calculate the acid capacity or equivalent weight of the membrane.
[b] Methanol permeability.
[c] The sample was immersed in distilled water at 60 °C for 1 h.

### 3.6. Methanol permeability

Fig. 8 plots the methanol permeability of Nafion® composite membranes fabricated with different silica–SH or oxidized silica–SH contents. The membrane thickness was maintained at about 120 μm by using the same total quantity of Nafion® and inorganic filler. The methanol permeability declined as the silica–SH content increased. The permeation of methanol normally occurs in clusters and ion-channels [30]. The silica–SH formed by a sol–gel reaction exist in the hydrophilic cluster and ion-channel, increasing the length of the path along which methanol permeates through the membrane. The methanol permeability of silica–$SO_3H$/Nafion® exceeded that of the silica–SH/Nafion® composite membrane. The methanol molecules transfer easily together with solvated protons ($H_3O^+$ or $H_5O_2^+$) because the hydrophilicity of the sulfonate groups of silica–$SO_3H$/Nafion® exceeds that of the silica–SH/Nafion® composite membrane. The methanol permeability of the silica–$SO_3H$/Nafion® composite membrane was still lower than the pristine Nafion®. Adding silica–SH and silica–$SO_3H$ to the membrane reduces the methanol permeability by approximately 30% and 15%, respectively.

The proton conductivity and the methanol crossover dominate the cell performance in a DMFC. Strong cell performance is associated with high proton conductivity and low methanol crossover. Adding silica–$SO_3H$ to the membrane increases the ratio of proton conductivity to methanol permeability (C/P ratio), as presented in Table 3.

### 3.7. DMFC test

The cell performance of composite membranes was tested in a DMFC single cell. Fig. 9 plots cell potential as a function of current density and power density versus current density for the DMFC membrane-electrode assembly (MEA) with a composite membrane with 0.6 wt% silica–$SO_3H$ and pristine Nafion®. Indeed, reducing the methanol crossover increases the open circuit voltage (OCV) and significantly improves the performance at low current densities. In this study, silica–SH/Nafion® and silica–$SO_3H$/Nafion® had higher OCVs than pristine Nafion®. However, pristine Nafion® outperformed silica–SH/Nafion® at lower current densities, perhaps because of the differences among the water uptake by the membranes. The changes in the water uptake may contribute to changes in the proton conductivity of the proton exchange membranes. Indeed, the incorporation of silica–SH was expected to enhance the hydrophobicity of the Nafion® membrane, reducing the water uptake, and the proton conductivity, reasonably explaining the cell performance at lower current densities. The composite membrane with 0.6 wt% silica–$SO_3H$/Nafion® outperformed pristine Nafion®. The current densities were measured as 62.5 and 70 mA cm$^{-2}$ at a potential of 0.2 V when the composite membrane contained 0 and 0.6 wt% silica–$SO_3H$, respectively.

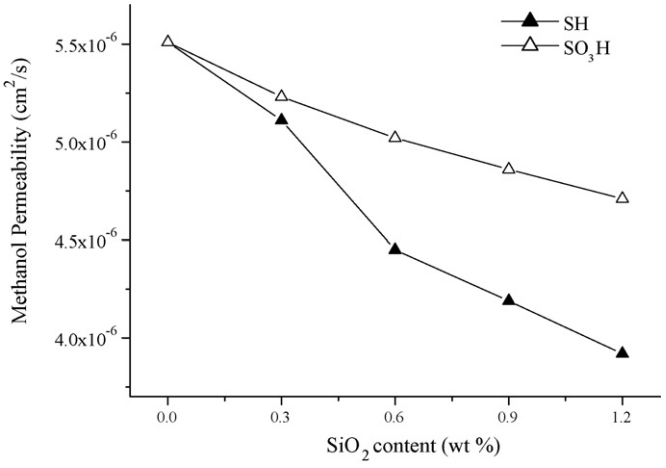


Fig. 8. The methanol permeability of silica–$SO_3H$/Nafion® and silica–SH/Nafion® on the various contents.

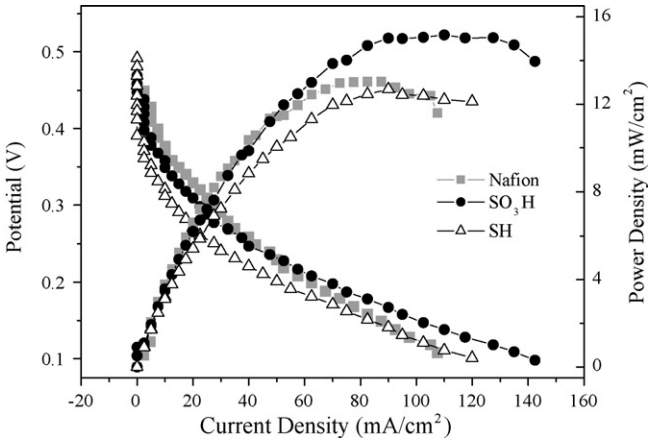


Fig. 9. Polarization curves for the MEA made with pristine Nafion® membrane and composite membranes operated at 313 K.

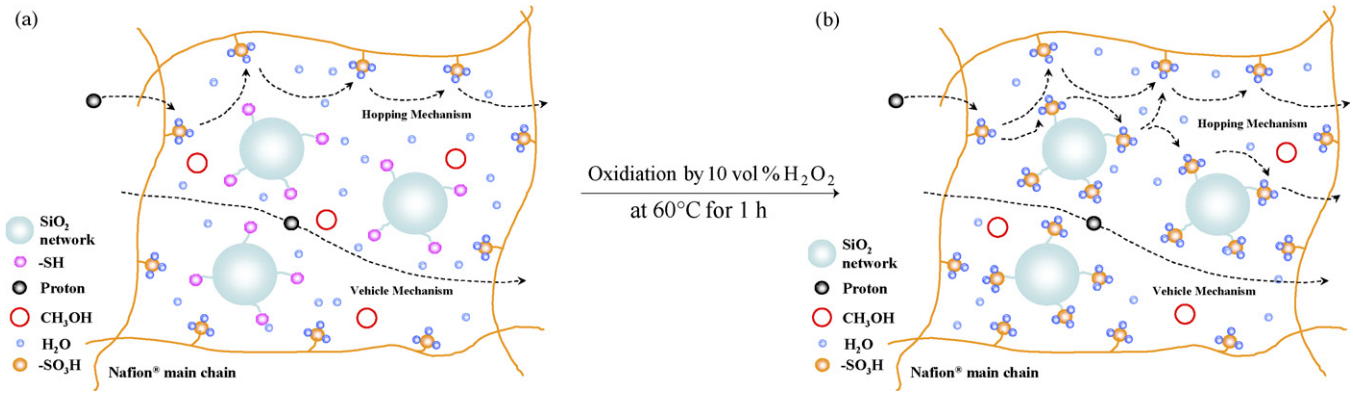


Scheme 1. The transport mechanism and structure of the (a) silica–SH/Nafion® and (b) silica–$SO_3H$/Nafion® composite membranes.

The current density of the silica–SH/Nafion® composite membrane was measured at 50 mA $cm^{-2}$ at a potential of 0.2 V. The cell performance of the DMFC was improved significantly by introducing silica–$SO_3H$. The maximum power density of 15.18 mW $cm^{-2}$ was obtained for the composite membrane with 0.6 wt% of silica–$SO_3H$; power density of pristine Nafion® was 13.04 mW $cm^{-2}$.

The presented silica–$SO_3H$/Nafion® system yields promising results for two reasons: (i) more sulfonic acid groups promote proton hopping, increasing the proton conductivity; (ii) silica in the composite membranes suppresses the crossover of the methanol Scheme 1.

## 4. Conclusions

Sulfonated-silica/Nafion® composite membranes were prepared successfully via the sol–gel reaction of SH-silane followed by oxidation with 10 wt% $H_2O_2$ solution. The XPS, $^{29}Si$ NMR and SEM results indicated that the optimum oxidation condition was 60 °C for 1 h. The performance of these silica–$SO_3H$/Nafion® composite membranes was evaluated in terms of methanol permeability, proton conductivity and cell performance. The proton conductivity of the composite membrane increased from 0.126 to 0.134 (S $cm^{-1}$) at a silica–$SO_3H$ content of 0.6 wt%. The methanol permeability of the composite membrane declined) as the silica–$SO_3H$ content in the composite membrane increased. The methanol permeability of the composite membrane that contained 0.6 wt% silica–$SO_3H$ was $5.02 \times 10^{-6}$ $cm^2$ $S^{-1}$, which was 10% less than that of pristine Nafion®. The Nafion®/0.6 wt% silica–$SO_3H$ composite membrane exhibited higher selectivity (C/P ratio = 26,653) than that of recasting Nafion® (C/P ratio = 22,795). The high selectivity indicates that the composite membrane is appropriate for DMFC applications. These effects markedly improve the performance of a DMFC made from Nafion®/silica–$SO_3H$ composite membranes.

## Acknowledgment

This work was supported by the Ministry of Economic Affairs.

## References

[1] B. Yang, A. Manthiram, Electrochem. Commun. 6 (2004) 231.
[2] S.P. Nunes, B. Ruffmann, E. Rikowski, S. Vetter, K. Richau, J. Membr. Sci. 203 (2002) 215.
[3] S. Tan, D. Bélanger, J. Phys. Chem. B 109 (2005) 23480.
[4] H.S. Park, Y.J. Kim, W.H. Hong, Y.S. Choi, H.K. Lee, Macromolecules 38 (2005) 2289–2295.
[5] B.C. Bae, H.Y. Ha, D.J. Kim, J. Membr. Sci. 276 (2006) 51–58.
[6] Z.X. Liang, T.S. Zhao, J. Phys. Chem. C 111 (2007) 8128–8134.
[7] Z.Q. Ma, P. Cheng, T.S. Zhao, J. Membr. Sci. 215 (2003) 327–336.
[8] J. Prabhuram, T.S. Zhao, Z.X. Liang, H. Yang, C.W. Wong, J. Electrochem. Soc. 152 (2005) A1390–A1397.
[9] Y.S. Kim, F. Wang, M. Hickner, T.A. Zawodzinski, J.E. McGrath, J. Membr. Sci. 212 (2003) 263.
[10] K.T. Adjemian, S.J. Lee, S. Srinivasan, J. Benziger, A.B. Bocarsly, J. Electrochem. Soc. 149 (3) (2002) A256.
[11] C. Li, G. Sun, S. Ren, J. Liu, Q. Wang, Z. Wu, H. Sun, W. Jin, J. Membr. Sci. 272 (2006) 50.
[12] T.M. Thampan, N.H. Jalani, P. Choi, R. Datta, J. Electrochem. Soc. 152 (2) (2005) A316.
[13] E. Chalkova, M.B. Pague, M.V. Fedkin, D.J. Wesolowski, S.N. Lvov, J. Electrochem. Soc. 152 (6) (2005) A1035.
[14] Y.F. Lin, C.Y. Yen, C.C.M. Ma, S.H. Liao, C.H. Hung, Y.H. Hsiao, J. Power Sources 165 (2007) 692–700.
[15] J.M. Thomassin, C. Pagnoulle, G. Caldarella, A. Germain, R. Jérôme, Polymer 46 (2005) 11389.
[16] C.H. Rhee, H.K. Kim, H. Chang, J.S. Lee, Chem. Mater. 17 (2005) 1691.
[17] P. Bébin, M. Caravanier, H. Galiano, J. Membr. Sci. 278 (2006) 35.
[18] H. Wang, B.A. Holmberg, L. Huang, Z. Wang, A. Mitra, J.M. Norbeck, Y. Yan, J. Mater. Chem. 12 (2002) 834.
[19] N. Miyake, J.S. Wainright, R.F. Savinell, J. Electrochem. Soc. 148 (2001) A898–A904.
[20] N. Miyake, J.S. Wainright, R.F. Savinell, J. Electrochem. Soc. 148 (2001) A905–A909.
[21] D.H. Jung, S.Y. Cho, D.H. Peck, D.R. Shin, J.S. Kim, J. Power Sources 106 (2002) 173–177.
[22] Q. Deng, R.B. Moore, K.A. Mauritz, J. Appl. Polym. Sci. 68 (1998) 747.
[23] N.H. Jalani, K. Dunn, R. Datta, Electrochim. Acta 51 (2005) 553–560.
[24] S. Ren, G. Sun, C. Li, Z. Liang, J. Membr. Sci. 282 (2006) 450–455.
[25] C.H. Rhee, Y.K. Kim, J.S. Lee, H.K. Kim, H. Chang, J. Power Sources 159 (2006) 1015–1024.
[26] Y.-F. Lin, C.-Y. Yen, C.-H. Hung, Y.-H. Hsiao, C.-C.M. Ma, J. Power Sources 168 (2007) 162–166.
[27] K.A. Mauritz, Mater. Sci. Eng. C-Bio. S. 6 (1998) 121–133.
[28] R.M. Sliverstein, F.X. Webster, Spectrometric Identification of Organic Compounds, 6th ed., wiley, New york, 1998.

[29] J.F. Moulder, W.F. Stickle, P.E. Sobol, K.D. Bomben, in: J. Chastain (Ed.), Handbook of X-ray Photoelectron Spectroscopy, Perkin-Elmer, Minnesota, 1992.
[30] R. Jiang, H. Russell Kunz, James M. Fenton, J. Membr. Sci. 272 (2006) 116–124.
[31] N.B. Colthup, L.H. Daly, S.E. Wiberley, Introduction to Infrared and Raman Spectroscopy, 3rd ed., Academic press, San Diego, 1990.
[32] Z.X. Liang, T.S. Zhao, J. Prabhuram, J. Membr. Sci. 283 (2006) 219–224.